DYNAMIC STIFFNESS VIBRATION ANALYSIS OF THICK SPHERICAL SHELL SEGMENTS WITH VARIABLE THICKNESS

Elia Efraim and Moshe Eisenberger

DYNAMIC STIFFNESS VIBRATION ANALYSIS OF THICK SPHERICAL SHELL SEGMENTS WITH VARIABLE THICKNESS

ELIA EFRAIM AND MOSHE EISENBERGER

A dynamic stiffness method is presented for determining the free vibration frequencies and mode shapes of thick spherical shell segments with variable thickness and different boundary conditions. The analysis uses the equations of the two-dimensional theory of elasticity, in which the effects of both transverse shear stresses and rotary inertia are accounted for. The displacement components are taken to be sinusoidal in time, periodic in the circumferential direction, constant through the thickness, and solved exactly in the meridional direction using the exact element method. The shape functions are derived from the exact solutions for the system of the differential equation of motion with variable coefficients. The dynamic stiffness matrix is derived from the exact shape functions and their derivatives. High-precision numerical results are presented for thick spherical shell segments with constant or linearly varying thickness and for several combinations of boundary conditions. Comparison is made with results of published research and with two- and three-dimensional finite element analyses.

1. Introduction

Spherical shells are extensively used in civil, mechanical, aircraft, and naval structures. The free vibration of solid and hollow spheres has been a subject of study for more than a century. Historical reviews of the research into the vibrations of spherical shell are given in [Leissa 1973; Kang and Leissa 2000; Qatu 2002]. For segmented spherical shells very few studies can be found. Gautham and Ganesan [1992] used finite elements to study the free vibration analysis of open spherical shells, based on a thick (two-dimensional) shell theory. A thick shell finite element was derived and vibration frequencies were obtained for spherical caps with and without center cutout having simply supported or clamped boundary conditions. Lim et al. [1996] analyzed spherical shells with variable thickness using two-dimensional shell theory and the Ritz method, and the results were compared with finite element and experimental ones. For spherical shell segments based on three-dimensional analysis, Kang and Leissa [2000] used the Ritz method to obtain accurate frequencies for thick spherical shell segments of uniform or varying thickness. Their method does not yield exact solutions, but with proper use of displacement components in the form of algebraic polynomials, one is able to obtain frequency upper bounds, that are as close to the exact values as desired. Corrected results for the test cases in that paper appeared subsequently in [Kang and Leissa 2006].

In this paper the equations of motion for a thick spherical shell segment with variable thickness are derived. Then, these are solved for the dynamic stiffness matrix of the segment, and assembled for a complete structure.

2. Equations of motion

The shell coordinates and shell parameters for axisymmetric spherical shells with thickness varying along the meridian are shown in Figure 1, left, where ϕ and θ are spherical angle coordinates, z is thickness coordinate from middle surface, R_0 is radius of curvatures of the middle surface of the shell in both meridian and circumferential directions and $R_p(\phi))$ describes the perpendicular distance to the axis of revolution of the generating line. The location of the shell segment is defined by either the angle of the beginning of the shell ϕ_b, or the angle of the end of the shell segment ϕ_e, and the meridional dimension of the shell is defined by the opening angle ϕ_0.
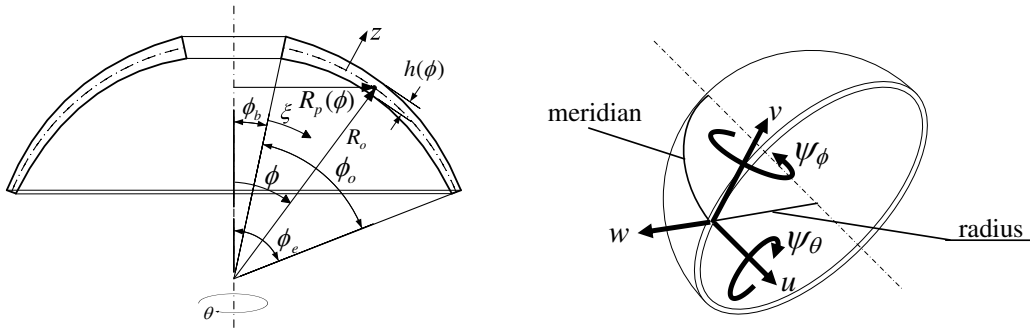

Figure 1. Left: geometry and coordinates of a spherical shell segment. Right: displacement field according to the thick shell theory.

The strain-displacement equations of the first order shear deformation shell theory of thick shells are obtained by satisfying the Kirchoff–Love hypothesis, such that normal to the shell mid-surface during deformation remain straight, and suffer no extension, but are not necessarily normal to the mid-surface after deformation. According to these assumptions the displacement of every point of the shell (see Figure 1, right) may be expressed as

$$
\begin{aligned}
u(\phi, \theta, z, t) &= U_0(\phi, \theta, t) + z \Psi_\phi(\phi, \theta, t), \\
v(\phi, \theta, z, t) &= V_0(\phi, \theta, t) + z \Psi_\theta(\phi, \theta, t), \\
w(\phi, \theta, z, t) &= W_0(\phi, \theta, t)
\end{aligned}
\tag{1}
$$

and the strain-displacement equations given in [Leissa and Chang 1996] for a general spherical shell become, for a spherical shell segment,

$$
\begin{aligned}
\epsilon_\phi &= \frac{\epsilon_{0\phi} + z k_\phi}{1 + z/R_0}, \quad \epsilon_\theta = \frac{\epsilon_{0\theta} + z k_\phi}{1 + z/R_0}, \\
\gamma_{\phi\theta} &= \frac{\gamma_{0\phi\theta} + z \tau_{\phi\theta} + \gamma_{0\theta\phi} + z \tau_{\theta\phi}}{1 + z/R_0}, \\
\gamma_{\phi z} &= \frac{\gamma_{0\phi z}}{1 + z/R_0}, \quad \gamma_{\theta z} = \frac{\gamma_{0\theta z}}{1 + z/R_0},
\end{aligned}
\tag{2}
$$

where we have denoted by $\epsilon_0.$, $\gamma_0..$ and $k.$ the strains and curvatures of the middle surface of the shell, given by the expressions

$$\epsilon_{0\phi} = \frac{1}{R_0}\frac{\partial U_0}{\partial \phi} + \frac{W_0}{R_0}, \qquad \epsilon_{0\theta} = \frac{1}{R_p}\frac{\partial V_0}{\partial \theta} + \frac{U_0}{R_0 R_p}\frac{\partial R_p}{\partial \phi} + \frac{W_0}{R_0},$$

$$k_\phi = \frac{1}{R_0}\frac{\partial \Psi_\phi}{\partial \phi}, \qquad k_\theta = \frac{1}{R_p}\frac{\partial \Psi_\theta}{\partial \theta} + \frac{\Psi_\phi}{R_0 R_p}\frac{\partial R_p}{\partial \phi},$$

$$\gamma_{0\phi\theta} = \frac{1}{A}\frac{\partial V_0}{\partial \phi}, \qquad \gamma_{0\theta\phi} = \frac{1}{R_p}\frac{\partial U_0}{\partial \theta} - \frac{V_0}{R_0 R_p}\frac{\partial R_p}{\partial \phi}, \qquad (3)$$

$$\gamma_{0\phi z} = \frac{1}{R_0}\frac{\partial W_0}{\partial \phi}\frac{U_0}{R_0} + \Psi_\phi, \quad \gamma_{0\phi z} = \frac{1}{R_p}\frac{\partial W_0}{\partial \theta} - \frac{V_0}{R_0} + \Psi_\theta.$$

Substituting the shell parameters into the five equations of motion of general shells [Leissa and Chang 1996] using the relations for principle shell coordinates ($\alpha_1 = \phi$, $\alpha_2 = \theta$), Lamé's coefficients ($A = R_0$, $B = R_p(\phi) = R_0 \sin \phi$) and radii of curvatures ($R_1 = R_2 = R_0$) yields the five equilibrium equations for a spherical shell segment with variable thickness:

$$\frac{dR_p(\phi)}{d\phi}N_\phi(\phi,\theta) + R_p(\phi)\frac{\partial N_\phi(\phi,\theta)}{\partial \phi} + R_0\frac{\partial N_{\theta\phi}(\phi,\theta)}{\partial \theta} - \frac{\partial R_p(\phi)}{\partial \phi}N_\theta(\phi,\theta)$$
$$+ R_0 R_p(\phi)Q_\phi(\phi,\theta) - R_p(\phi)\left(R_0 I_1(\phi)\ddot{U}_0(\phi,\theta,t) + 2I_3(\phi)\ddot{\Psi}_\phi(\phi,\theta,t)\right) = 0,$$

$$R_0\frac{\partial N_\theta(\phi,\theta)}{\partial \theta} + \frac{dR_p(\phi)}{d\phi}N_{\phi\theta}(\phi,\theta) + R_p(\phi)\frac{\partial N_{\phi\theta}(\phi,\theta)}{\partial \phi} + \frac{dR_p(\phi)}{d\phi}N_{\theta\phi}(\phi,\theta)$$
$$+ R_p(\phi)Q_\phi(\phi,\theta) - R_p(\phi)\left(R_0 I_1(\phi)\ddot{V}_0(\phi,\theta,t) + 2I_3(\phi)\ddot{\Psi}_\theta(\phi,\theta,t)\right) = 0,$$

$$-R_p(\phi)N_\phi(\phi,\theta) - R_p(\phi)N_\theta(\phi,\theta) + \frac{\partial R_p(\phi)}{\partial \phi}Q_\phi(\phi,\theta)$$
$$+ R_p(\phi)\frac{\partial Q_\phi(\phi,\theta)}{\partial \phi} + R_0\frac{\partial Q_\theta(\phi,\theta)}{\partial \theta} - R_0 R_p(\phi)I_1(\phi)\ddot{W}_0(\phi,\theta,t) = 0, \qquad (4)$$

$$\frac{dR_p(\phi)}{d\phi}M_\phi(\phi,\theta) + R_p(\phi)\frac{\partial M_\phi(\phi,\theta)}{\partial \phi} + R_0\frac{\partial M_{\theta\phi}(\phi,\theta)}{\partial \theta} - \frac{\partial R_p(\phi)}{\partial \theta}M_\theta(\phi,\theta)$$
$$- R_0 R_p(\phi)Q_\phi(\phi,\theta) - R_p(\phi)\left(2I_3(\phi)\ddot{U}_0(\phi,\theta,t) + R_0(\phi)I_3(\phi)\ddot{\Psi}_\phi(\phi,\theta,t)\right) = 0,$$

$$R_0\frac{\partial M_\theta(\phi,\theta)}{\partial \theta} + \frac{dR_p(\phi)}{d\phi}M_{\phi\theta}(\phi,\theta) + R_p(\phi)\frac{\partial M_{\phi\theta}(\phi,\theta)}{\partial \phi} + \frac{\partial R_p(\phi)}{\partial \phi}M_{\theta\phi}(\phi,\theta)$$
$$- R_0 R_p(\phi)Q_\phi(\phi,\theta) - R_p(\phi)\left(2I_3(\phi)\ddot{V}_0(\phi,\theta,t) + R_0 I_3(\phi)\ddot{\Psi}_\theta(\phi,\theta,t)\right) = 0.$$

with variable quantities $I_1(\phi)$, $I_3(\phi)$ obtained by integration of the material density through the thickness as follows:

$$I_1(\phi) = \int_{-h(\phi)/2}^{+h(\phi)/2} \rho \, dz = \rho h(\phi), \qquad I_3(\phi) = \int_{-h(\phi)/2}^{+h(\phi)/2} \rho z^2 \, dz = \frac{\rho h^3(\phi)}{12}. \qquad (5)$$

The stress-strain relations for an isotropic material are given by

$$
\left\{
\begin{array}{c}
\sigma_\phi \\
\sigma_\theta \\
\sigma_{\phi\theta} \\
\sigma_{\phi z} \\
\sigma_{\theta z}
\end{array}
\right\}
= \frac{E}{1-\mu^2}
\begin{bmatrix}
1 & \mu & 0 & 0 & 0 \\
\mu & 1 & 0 & 0 & 0 \\
0 & 0 & (1-\mu)/2 & 0 & 0 \\
0 & 0 & 0 & (1-\mu)/2 & 0 \\
0 & 0 & 0 & 0 & (1-\mu)/2
\end{bmatrix}
\left\{
\begin{array}{c}
\epsilon_\phi \\
\epsilon_\theta \\
\gamma_{\phi\theta} \\
\gamma_{\phi z} \\
\gamma_{\theta z}
\end{array}
\right\},
\tag{6}
$$

where E is the modulus of elasticity and μ is Poisson's ratio. For isotropic materials the force and moment resultants are obtained by integrating the stresses through the shell thickness, which in this case is variable along the meridian:

$$
\left\{
\begin{array}{c}
N_\phi(\phi,\theta) \\
N_\theta(\phi,\theta) \\
N_{\phi\theta}(\phi,\theta) \\
N_{\theta\phi}(\phi,\theta)
\end{array}
\right\}
= \int_{-h(\phi)/2}^{+h(\phi)/2}
\left\{
\begin{array}{c}
\sigma_\phi(z) \\
\sigma_\theta(z) \\
\sigma_{\phi\theta}(z) \\
\sigma_{\theta\phi}(z)
\end{array}
\right\}
\left(1 + \frac{z}{R_0}\right) dz,
\tag{7}
$$

$$
\left\{
\begin{array}{c}
Q_\phi(\phi,\theta) \\
Q_\theta(\phi,\theta)
\end{array}
\right\}
= \kappa \int_{-h(\phi)/2}^{+h(\phi)/2}
\left\{
\begin{array}{c}
\sigma_{\phi z}(z) \\
\sigma_{\theta z}(z)
\end{array}
\right\}
\left(1 + \frac{z}{R_0}\right) dz,
\tag{8}
$$

$$
\left\{
\begin{array}{c}
M_\phi(\phi,\theta) \\
M_\theta(\phi,\theta) \\
M_{\phi\theta}(\phi,\theta) \\
M_{\theta\phi}(\phi,\theta)
\end{array}
\right\}
= \int_{-h(\phi)/2}^{+h(\phi)/2}
\left\{
\begin{array}{c}
\sigma_\phi(z) \\
\sigma_\theta(z) \\
\sigma_{\phi\theta}(z) \\
\sigma_{\theta\phi}(z)
\end{array}
\right\}
\left(1 + \frac{z}{R_0}\right) z\, dz,
\tag{9}
$$

where κ is a shear correction factor. Various derivations of the shear correction factor have been proposed. Mindlin [1951] gave an implicit result for the shear correction factor for isotropic elastic plates that depends on Poisson ratio μ. Hutchinson [1984] determined the shear coefficient in a Mindlin plate equation based on matching a mode of the Mindlin plate theory to the exact Rayleigh–Lamb frequency equation for the flexural wave response at long wavelengths and proposed the value $\kappa = 5/(6-\mu)$. Later, Stephen [1997] reexamined this solution, and called this the "best" shear coefficient. In the present work this value of Hutchinson's shear coefficient is used in the calculations.

Considering the stress-strain relations, the kinematical relations for shells with variable thickness the constitutive relations become

$$
N_\phi(\phi,\theta) = \frac{E}{1-\mu^2} h(\phi)(\epsilon_{0\phi} + \mu\epsilon_{0\theta}), \qquad N_\theta(\phi,\theta) = \frac{E}{1-\mu^2} h(\phi)(\mu\epsilon_{0\phi} + \epsilon_{0\theta}),
$$

$$
Q_\phi(\phi,\theta) = \frac{\kappa E}{2(1+\mu)} h(\phi)\gamma_{0\phi n}, \qquad Q_\theta(\phi,\theta) = \frac{\kappa E}{2(1+\mu)} h(\phi)\gamma_{0\phi n},
$$

$$
N_{\phi\theta}(\phi,\theta) = \frac{E}{2(1+\mu)} h(\phi)(\gamma_{0\phi\theta} + \gamma_{0\theta\phi}), \qquad N_{\theta\phi}(\phi,\theta) = N_{\phi\theta}(\phi,\theta),
\tag{10}
$$

$$
M_\phi(\phi,\theta) = \frac{E}{1-\mu^2} \frac{h^3(\phi)}{12}(k_\phi + \mu k_\theta), \qquad M_\theta(\phi,\theta) = \frac{E}{1-\mu^2} \frac{h^3(\phi)}{12}(\mu k_\phi + k_\theta),
$$

$$
M_{\phi\theta}(\phi,\theta) = \frac{E}{2(1+\mu)} \frac{h^3(\phi)}{12}(\tau_{\phi\theta} + \tau_{\theta\phi}), \qquad M_{\theta\phi}(\phi,\theta) = M_{\phi\theta}(\phi,\theta).
$$

3. Solution procedure

We introduce a nondimensional coordinate $\xi = (\phi - \phi_b)/\phi_0$ that vary from 0 to 1. The variation of the geometric parameters h and R_p is taken in a polynomial form as follows:

$$h(\phi) \implies h(\xi) = \sum_{i=0}^{nh} h_i \xi^i, \qquad R_p(\phi) \implies R_p(\xi) = \sum_{i=0}^{nR_p} R_{pi} \xi^i, \tag{11}$$

Spherical shell segments with a wide range of meridian opening angles, concave or convex thickness variation can be described in this way, up to any desired accuracy. In case of shell with wavy or corrugated surface, it could be represented by segmented shell with sequential shell segments with convex and concave thickness variation.

When the force and moment resultants are substituted into the equations of motion (4), assuming harmonic vibrations, and using the assumed displacement field

$$U_0(\phi, \theta, t) = u(\phi) \cos n\theta \sin \omega t,$$
$$V_0(\phi, \theta, t) = v(\phi) \sin n\theta \sin \omega t,$$
$$W_0(\phi, \theta, t) = w(\phi) \cos n\theta \sin \omega t,$$
$$\Psi_\phi(\phi, \theta, t) = \psi_\phi(\phi) \cos n\theta \sin \omega t, \tag{12}$$
$$\Psi_\theta(\phi, \theta, t) = \psi_\theta(\phi) \sin n\theta \sin \omega t,$$

with the notation

$$\boldsymbol{U}(\phi) = \{u(\phi), v(\phi), w(\phi), \psi_\phi(\phi), \psi_\theta(\phi)\}^T \tag{13}$$
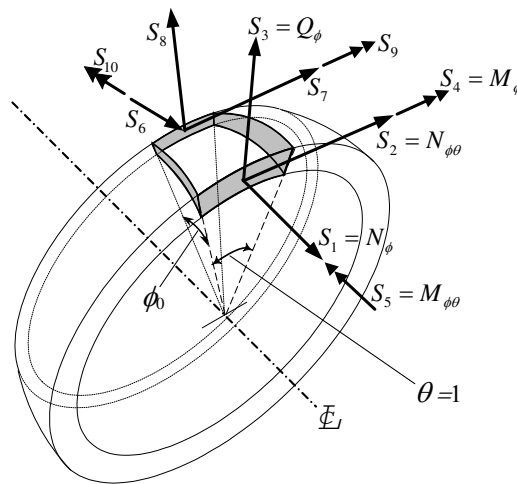

Figure 2. Dynamic stiffnesses defined by resultant forces along a unit angle segment of the perimeter of the shell edges ($\xi = 0$, $\xi = 1$).

after transformation to the nondimensional coordinate ξ, we obtain the equations of motion in term of the displacements as

$$K^{(0)}(\xi, \omega)U(\xi) + K^{(1)}(\xi)U'(\xi) + K^{(2)}(\xi)U''(\xi) = 0, \tag{14}$$

where primes refer to derivatives with respect to ξ, and the terms in the matrices $K^{(0)}$, $K^{(1)}$, and $K^{(2)}$ are given in the Appendix. The solution is obtained using the exact element method algorithm [Eisenberger 1990] by assuming the solution as infinite power series

$$U(\xi) = \sum_{i=0}^{\infty} u_i \xi^i, \tag{15}$$

and following the procedure in [Eisenberger 1990] we get the five basic shape functions for each case of unit displacement on the shell edges. Based on the values of the shape functions and their derivatives at the two edges of the segment ($\xi = 0; \xi = 1$) we get the terms in the dynamic stiffness matrix as the resultant forces along the unit angle segment of the perimeter of the shell, as shown in Figure 2, as

$$
\begin{aligned}
\left.\begin{array}{c} S_1 \\ S_6 \end{array}\right\} &= N_\phi\bigg|_{\substack{\xi=0\\\xi=1}} = \frac{E}{1-\mu^2}\left[\frac{R'_p\Phi}{R_0}\mu u + \frac{R_p\Phi}{R_0}u' + \mu n v + \left(\frac{R_p}{R_0}(1+\mu)\right)w\right]\bigg|_{\substack{\xi=0\\\xi=1}}, \\[2mm]
\left.\begin{array}{c} S_2 \\ S_7 \end{array}\right\} &= N_{\phi\theta}\bigg|_{\substack{\xi=0\\\xi=1}} = \frac{E}{2(1+\mu)}\left[-nu - \frac{R'_p\Phi}{R_0}v + \frac{R_p\Phi}{R_0}v'\right]\bigg|_{\substack{\xi=0\\\xi=1}}, \\[2mm]
\left.\begin{array}{c} S_3 \\ S_8 \end{array}\right\} &= Q_\phi\bigg|_{\substack{\xi=0\\\xi=1}} = \frac{\kappa E}{2(1+\mu)}\left[-\frac{R_p}{R_0}u + \frac{R_p\Phi}{R_0}w' + \psi_s\right]\bigg|_{\substack{\xi=0\\\xi=1}}, \\[2mm]
\left.\begin{array}{c} S_4 \\ S_9 \end{array}\right\} &= M_\phi\bigg|_{\substack{\xi=0\\\xi=1}} = \frac{E}{(1-\mu^2)}\frac{h^3}{12}\left[\mu\frac{R'_p\Phi}{R_0}\psi_\phi + \frac{R_p\Phi}{R_0}\psi'_\phi + \mu n\psi_\phi\right]\bigg|_{\substack{\xi=0\\\xi=1}}, \\[2mm]
\left.\begin{array}{c} S_5 \\ S_{10} \end{array}\right\} &= M_{\phi\theta}\bigg|_{\substack{\xi=0\\\xi=1}} = \frac{E}{2(1+\mu)}\frac{h^3}{12}\left[-n\psi_\phi - \frac{R'_p\Phi}{R_0}\psi_\theta + \left(\frac{R_p}{R_0}\right)\Phi\psi'_\theta\right]\bigg|_{\substack{\xi=0\\\xi=1}}.
\end{aligned}
\tag{16}
$$

The dynamic stiffness matrix for a segment, having ten degrees of freedom, five on each edge, is then assembled for the structure in the usual procedure of structural analysis. The natural frequencies of vibration are found as the values of the frequency that will cause the assembled dynamic stiffness matrix of the structure to become singular.

When the cut-outs size becomes relatively small ($R_{p,\text{in}}/R_{p,\text{out}} < 0.1$) the shape functions series converges rather slowly and have relatively large number of terms. Therefore, in order speed the convergence process one can divide the shell into sections with ratio $R_{p,\text{in}} = 0.3R_{p,\text{out}}$ for each section. So, by adding a small number of elements one can solve for shells with very small cut-outs (e.g., three elements for $R_{p,\text{in}} = 0.03R_{p,\text{out}}$ and four elements for $R_{p,\text{in}} = 0.01R_{p,\text{out}}$).

4. Numerical examples

In order to obtain a high-precision solution for vibration problems of thick spherical shells, numerical calculations have been performed for a spherical shells with different thickness-radius ratios, and various

| | $h/R = 0.1$ | | | | | | $h/R = 0.2$ | | | | | |
| | Clamped-Free | | | SS-Free | | | Clamped-Free | | | SS-Free | | |
n	5 DOF	Lit.	Diff.%	7 DOF	Lit.	Diff.%	5 DOF	Lit.	Diff.%	7 DOF	Lit.	Diff.%
0	0.9810	0.978	0.30	0.9079	0.906	0.21	1.1403	1.133	0.64	1.0516	1.047	0.44
	1.3025	1.297	0.42	1.3025	1.297	0.42	1.3025	1.297	0.42	1.3022	1.297	0.40
	1.3398	1.340	–0.01	1.3398	1.340	–0.02	1.4212	1.427	–0.40	1.3583	1.358	0.02
1	0.7052	0.704	0.17	0.6593	0.658	0.19	0.7553	0.753	0.30	0.6785	0.678	0.08
	1.0757	1.073	0.25	1.0172	1.014	0.32	1.2999	1.295	0.38	1.2065	1.203	0.29
	1.6828	1.684	–0.07	1.5745	1.572	0.16	1.9858	1.982	0.19	1.9829	1.965	0.91
2	0.4477	0.445	0.61	0.4111	0.409	0.51	0.6530	0.653	0.00	0.5687	0.571	–0.41
	1.2783	1.275	0.26	1.1921	1.185	0.60	1.6917	1.688	0.22	1.5586	1.550	0.56
	1.8342	1.835	–0.05	1.7248	1.722	0.16	2.0241	2.022	0.10	2.0181	2.007	0.55
3	0.7617	0.764	–0.30	0.7453	0.747	–0.23	1.1415	1.157	–1.34	1.0726	1.086	–1.24
	1.4676	1.465	0.17	1.3656	1.357	0.63	2.0931	2.087	0.29	1.9374	1.922	0.80
	2.1411	2.142	–0.04	1.9834	1.979	0.22	2.4381	2.435	0.13	2.4306	2.428	0.11
4	1.1698	1.176	–0.52	1.1406	1.145	–0.38	1.6949	1.719	–1.40	1.6041	1.622	–1.11
	1.7184	1.718	0.02	1.6085	1.602	0.41	2.5572	2.557	0.01	2.4219	2.426	–0.17
	2.4824	**2.776**	**–10.6**	2.3148	2.311	0.17	3.1124	3.107	0.17	3.0877	3.087	0.02
5	1.5177	1.525	–0.48	1.4576	1.461	–0.23	2.2095	2.235	–1.14	2.0996	2.118	–0.87
	2.1060	2.109	–0.14	1.9964	1.994	0.12	3.1445	3.151	-0.21	3.0215	3.024	–0.08
	2.8804	2.885	–0.16	2.7240	2.721	0.11	3.8489	3.860	–0.29	3.8133	3.851	–0.98

Table 1. Nondimensional frequency $\lambda = \omega R \sqrt{\rho/E}$ for a hemispherical shell with a 30°
cutout at the apex, with free boundary conditions at the cutout and different boundary
conditions at the base. The columns "5 DOF" and "7 DOF" give the result with the
present method (one exact element and the specified number of degrees of freedom).
"Lit." refers to [Gautham and Ganesan 1992]. "Diff.%" is the ratio $(\lambda_{\text{exact}} - \lambda_{\text{FE}})/\lambda_{\text{FE}}$.

combinations of boundary conditions: constant thickness hemispherical caps with annular cutout at the
apex, variable thickness spherical annular segment, and variable thickness spherical barrel shell.

The results for the constant thickness hemispherical shells are set out in Tables 1 and 2 for two
cutout sizes (60° and 30°), and with two types of boundary conditions at the base: clamped and simply
supported, and two thickness/radius ratios: 0.1 and 0.2. A comparison is made with the results of the FE
analysis of [Gautham and Ganesan 1992] that were obtained by using Nagdhi's basic relations that take
the transverse shear and the normal strain into consideration. Three-noded finite elements with 7 DOF
per node were used for solving the problem. Good general agreement of the results is shown. Some
fictitious frequencies given by FE analysis can be observed (marked in bold).

Table 3, left, presents a comparison of the natural frequencies for an annular hemispherical shell
with linearly varying thickness ($\phi_0 = 60°$, $h_b/h_e = 1/3$) (Figure 3, left). The comparison is performed
with the results from FE analysis using the commercial code ABAQUS, and the results from a three-
dimensional analysis by the Ritz method reported in [Kang and Leissa 2006]. The results of the present

| | $h/R = 0.1$ | | | | | | $h/R = 0.2$ | | | | | |
| | Clamped-Free | | | SS-Free | | | Clamped-Free | | | SS-Free | | |
n	5 DOF	Lit.	Diff.%	7 DOF	Lit.	Diff.%	5 DOF	Lit.	Diff.%	7 DOF	Lit.	Diff.%
0	1.1353	1.139	–0.32	1.0722	1.072	0.02	1.2777	1.289	–0.88	1.0583	1.059	–0.06
	2.0232	2.014	0.45	1.7280	1.726	0.12	2.0232	2.013	0.50	2.0223	2.014	0.41
	2.1232	2.125	–0.08	2.0231	2.010	0.65	2.7504	2.747	0.12	2.4947	2.487	0.31
1	0.9833	0.984	–0.07	0.8890	0.887	0.22	1.1492	1.152	–0.24	0.8968	0.895	0.20
	2.1026	2.106	–0.16	1.7584	1.756	0.14	2.3395	2.337	0.11	2.3347	2.332	0.12
	2.4140	2.408	0.25	2.3790	2.369	0.42	2.8142	2.810	0.15	2.5781	2.565	0.51
2	0.7965	0.794	0.32	0.6507	0.648	0.41	1.0567	1.053	0.35	0.7540	0.751	0.40
	2.2267	2.232	–0.24	1.8775	**2.038**	**–7.88**	2.8075	2.822	-0.51	2.6616	2.670	–0.31
	3.0967	3.088	0.28	3.0846	**2.764**	**11.6**	3.1626	3.150	0.40	3.1131	3.087	0.85
3	0.7515	0.748	0.47	0.5844	0.581	0.58	1.1578	1.154	0.33	0.8790	0.879	0.00
	2.4119	2.416	–0.17	2.0644	**2.522**	**–18.1**	3.0761	3.099	-0.74	2.9268	2.939	–0.42
	3.3919	3.398	–0.18	3.3843	**2.524**	**34.1**	3.6591	3.634	0.69	3.5337	3.459	2.16
4	0.8764	0.873	0.39	0.7344	0.731	0.47	1.4400	1.441	–0.07	1.2250	1.230	–0.40
	2.6411	2.643	–0.07	2.2964	2.307	–0.46	3.3779	3.407	–0.85	3.2616	3.278	–0.50
	3.5287	3.532	–0.09	3.5250	3.477	1.38	3.8222	3.782	1.06	3.6590	3.586	2.03
5	1.1272	1.126	0.11	1.0160	1.014	0.20	1.8473	1.853	–0.31	1.6855	1.693	–0.44
	2.8959	2.894	0.06	2.5589	2.546	0.51	3.7419	3.772	–0.80	3.6600	3.675	–0.41
	3.7873	3.789	–0.04	3.7869	3.780	0.18	4.0686	4.025	1.08	3.8853	3.818	1.76

Table 2. Nondimensional frequency $\lambda = \omega R \sqrt{\rho/E}$ for hemispherical shells with 60°
cutout at the apex, with free boundary conditions at the cutout and different boundary
conditions at the base. The columns "5 DOF" and "7 DOF" give the result with the
present method (one exact element and the specified number of degrees of freedom).
"Lit." refers to [Gautham and Ganesan 1992]. "Diff.%" is the ratio $(\lambda_{\text{exact}} - \lambda_{\text{FE}})/\lambda_{\text{FE}}$.
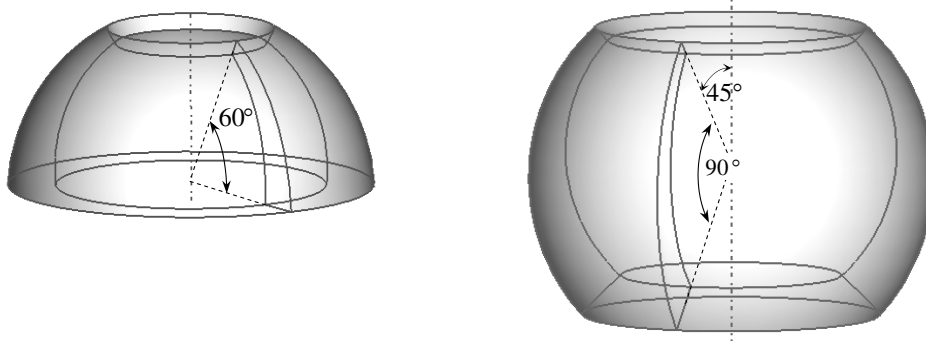

Figure 3. Left: hemispherical annular shell with linearly varying thickness; $\phi_0 = 60°$,
$h_b/h_e = 1/3$ (results in Table 3, left). Right: spherical barrel shell with variable thick-
ness; $\phi_b = 45°$, $\phi_e = 135°$, $(h_b + h_e)/2R = 0.2$, $h_b/h_e = 1/3$, $\mu = 0.3$ (results in Table 3,
right, and Figures 4–7).

n	2D FE 1600 S4R shell els. 10080 DOF	3D FE 2095 C3D20R solid els. 43020 DOF	[Kang and Leissa 2006] 3D, Ritz	Present DSM with 2 exact els. 15 DOF	3D FE 2095 C3D20R solid els. 43020 DOF	[Kang and Leissa 2006] 3D, Ritz	Present DSM with 3 exact els. 20 DOF
0 (A)	1.5357	1.5361	1.536	1.5347	1.5345	1.535	1.5299
	2.1152	2.0862	2.090	2.1138	1.9099	1.911	1.9268
	2.3992	2.4216	2.423	2.4057	1.9632	1.963	1.9651
	4.3117	4.3143	4.322	4.3041	2.4772	2.487	2.4846
	5.9909	5.8511	5.844	5.9780	3.8292	3.844	3.8355
0 (T)	3.7144	3.6775	3.669	3.7053	2.4774	2.470	2.4938
	6.5151	6.3843	6.385	6.4586	4.2877	4.290	4.3343
	9.5088	9.1976	9.200	9.3248	6.1689	6.172	6.2411
					NA	8.093	8.1862
1	1.5666	1.5687	1.568	1.5645	1.3915	1.390	1.3898
	2.4016	2.3730	2.374	2.3990	1.7690	1.771	1.7688
	2.4824	2.4819	2.485	2.4845	2.3793	2.379	2.4037
	4.4149	4.4072	4.414	4.4101	2.5836	2.594	2.5915
	4.6268	4.5782	4.572	4.6131	3.4497	3.445	3.4897
2	0.3495	0.3495	0.349	0.3494	0.3593	0.362	0.3613
	0.7135	0.7031	0.705	0.7136	0.6065	0.604	0.6076
	1.8514	1.8563	1.857	1.8443	1.6842	1.690	1.6977
	2.8071	2.8044	2.809	2.8093	2.0238	2.027	2.0281
	3.6503	3.5714	3.572	3.6372	2.8902	2.901	2.9006
3	0.9382	0.9368	0.934	0.9364	0.9085	0.918	0.9169
	1.6815	1.6615	1.666	1.6794	1.4032	1.400	1.3997
	2.6617	2.6422	2.646	2.6436	2.2845	2.298	2.3155
	3.3486	3.3397	3.346	3.3494	2.6510	2.651	2.6687
	4.8367	4.7495	4.746	4.8121	3.3737	3.385	3.3824
4	1.6823	1.6757	1.671	1.6753	1.5436	1.561	1.5597
	2.6672	2.6368	2.643	2.6577	2.1947	2.196	2.1917
	3.6246	3.5577	3.564	3.5878	2.9024	2.911	2.9192
	4.0553	4.0540	4.060	4.0547	3.5713	3.579	3.6300
	5.8216	5.8013	5.793	5.8063	4.0506	4.059	4.0507
5	2.5319	2.5140	2.507	2.5144	2.2465	2.271	2.2696
	3.6775	3.6304	3.637	3.6558	2.9445	2.954	2.9478
	4.5940	4.4686	4.475	4.5297	3.6991	3.707	3.7014
	4.9368	4.9436	4.951	4.9250	4.4644	4.477	4.5276
	6.6094	6.6536	6.665	6.6166	4.9457	4.952	4.9700

Table 3. Comparison of the nondimensional natural frequency $\Omega = \omega R \sqrt{\rho/G}$ for completely free spherical shells with linearly varying thickness. Left: annular shell with $\phi_b = 30°$ and $\phi_e = 90°$ (Figure 3, left). Right: barrel shell with $\phi_b = 45°$ and $\phi_e = 135°$ (Figure 3, right). In both cases, $(h_b + h_e)/2R = 0.2$, $h_b/h_e = 1/3$, and $\mu = 0.3$. "A" stands for axisymmetric modes, "T" for torsional modes.
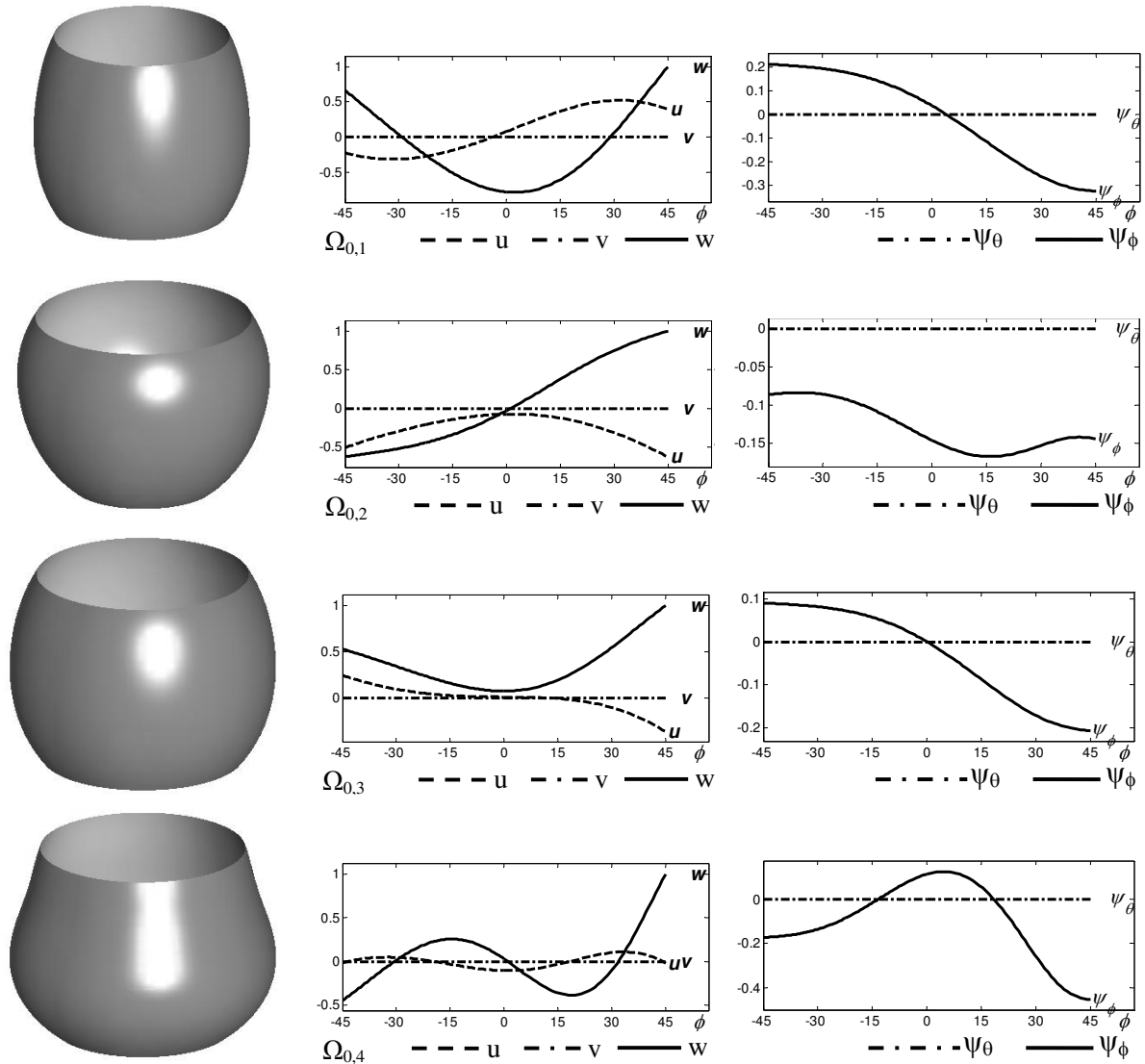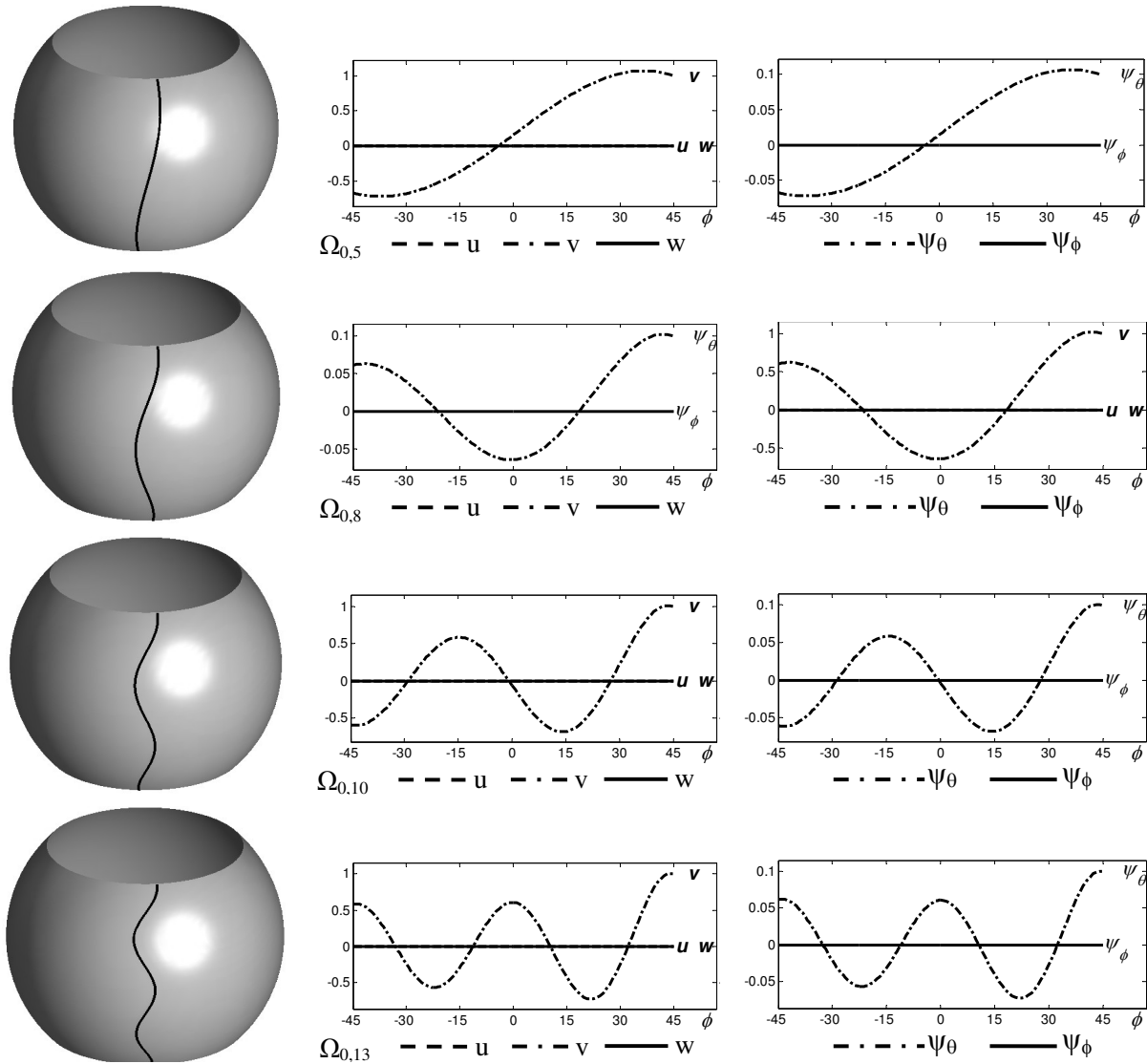
Figure 4. The first four mode shapes of axisymmetric vibrations ($n = 0$) of completely
free spherical barrel shell with variable thickness (Figure 3, right).

exact analysis are generally lower than the results from the two-dimensional FE analysis, and for some
modes the frequency is a little bit higher due the difference in the shear correction factor that was used:
$5/(6 - \mu)$ in the present analysis versus $5/6$ in the FE analysis. Comparison with the three-dimensional
Ritz solution shows that the torsional modes in the present analysis are higher than the values in the
three-dimensional analysis due to kinematical simplifications of the first order shear deformation shell
theory. In other vibrational modes no clear tendency is observed.

The same conclusions are obtained from comparison of frequency results for barrel spherical shell
($\phi_b = 45°$, $\phi_e = 135°$, $(h_b + h_e)/2R = 0.2$, $h_b/h_e = 1/3$, $\mu = 0.3$) presented in Table 3, right. Figures 4,

Figure 5. The first four mode shapes of pure torsional vibrations ($n = 0$) of completely free spherical barrel shell with variable thickness (Figure 3, right).

5, 6, and 7 show the three-dimensional vibrational modes and the exact displacement shape functions obtained by the present method.

5. Conclusions

The natural frequencies for spherical shells of revolution with different boundary conditions have been investigated using the Dynamic Stiffness method. This approach is combined with the exact element method for the vibration analysis of spherical shell segments with curved meridian and variable cross-section. The analysis uses the equations of the two-dimensional theory of elasticity, in which the effects
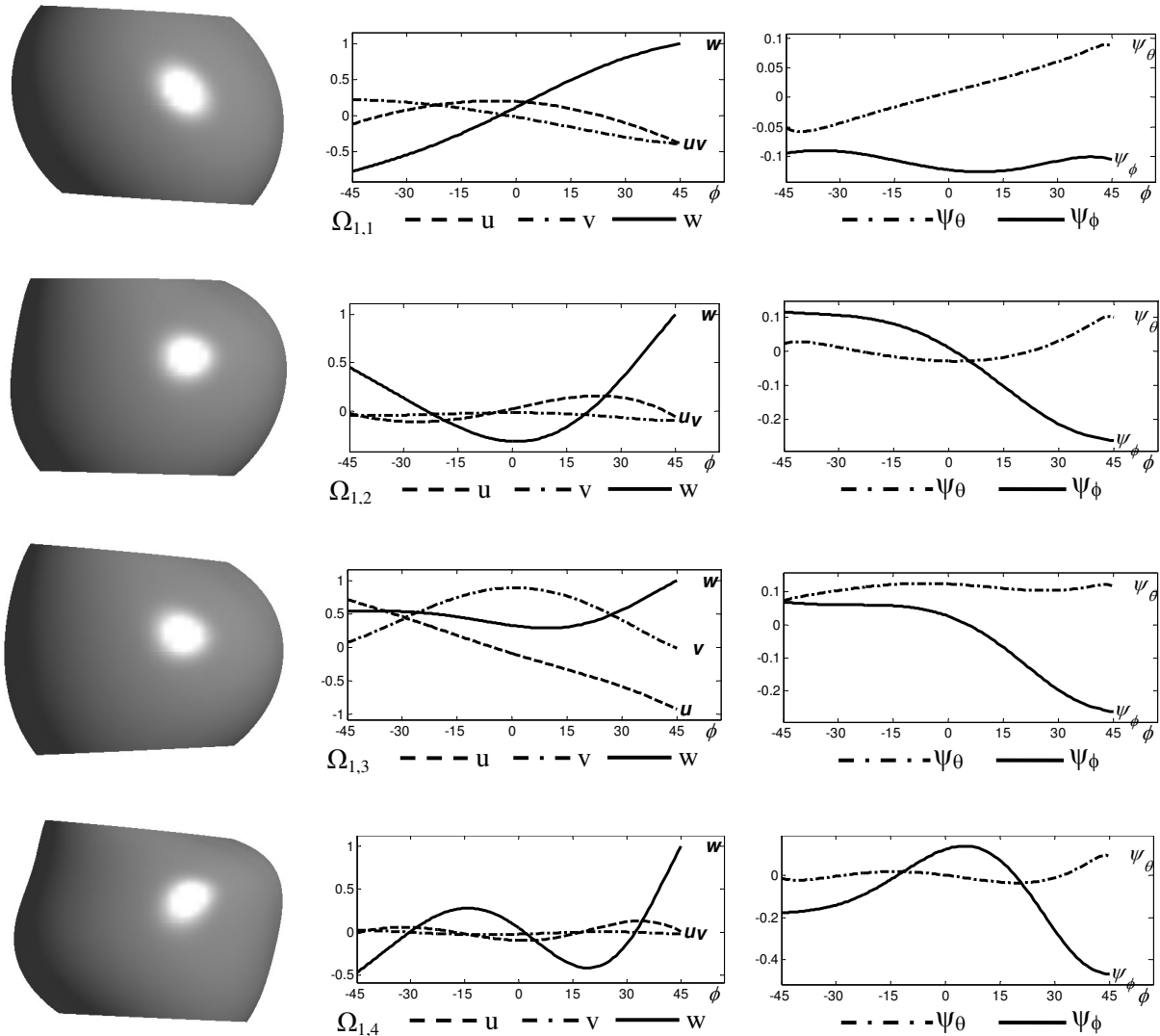
Figure 6. Mode shapes of vibrations with one circumferential waves ($n = 1$) of a completely free spherical barrel shell with variable thickness (Figure 3, right).

of both transverse shear stresses and rotary inertia are accounted for, in their general forms for isotropic homogeneous materials. The proposed method shows the following advantages:

(1) Any polynomial variation of the thickness of the shell along the meridian can be considered.

(2) The method is mesh-free, and dividing the surface to many elements doesn't improve the solution. No convergence study is necessary to obtain the true results.

(3) The shape functions are derived automatically and they are the exact solutions for the system of the differential equation of motion with variable coefficients. As a result, the solution for free vibrations
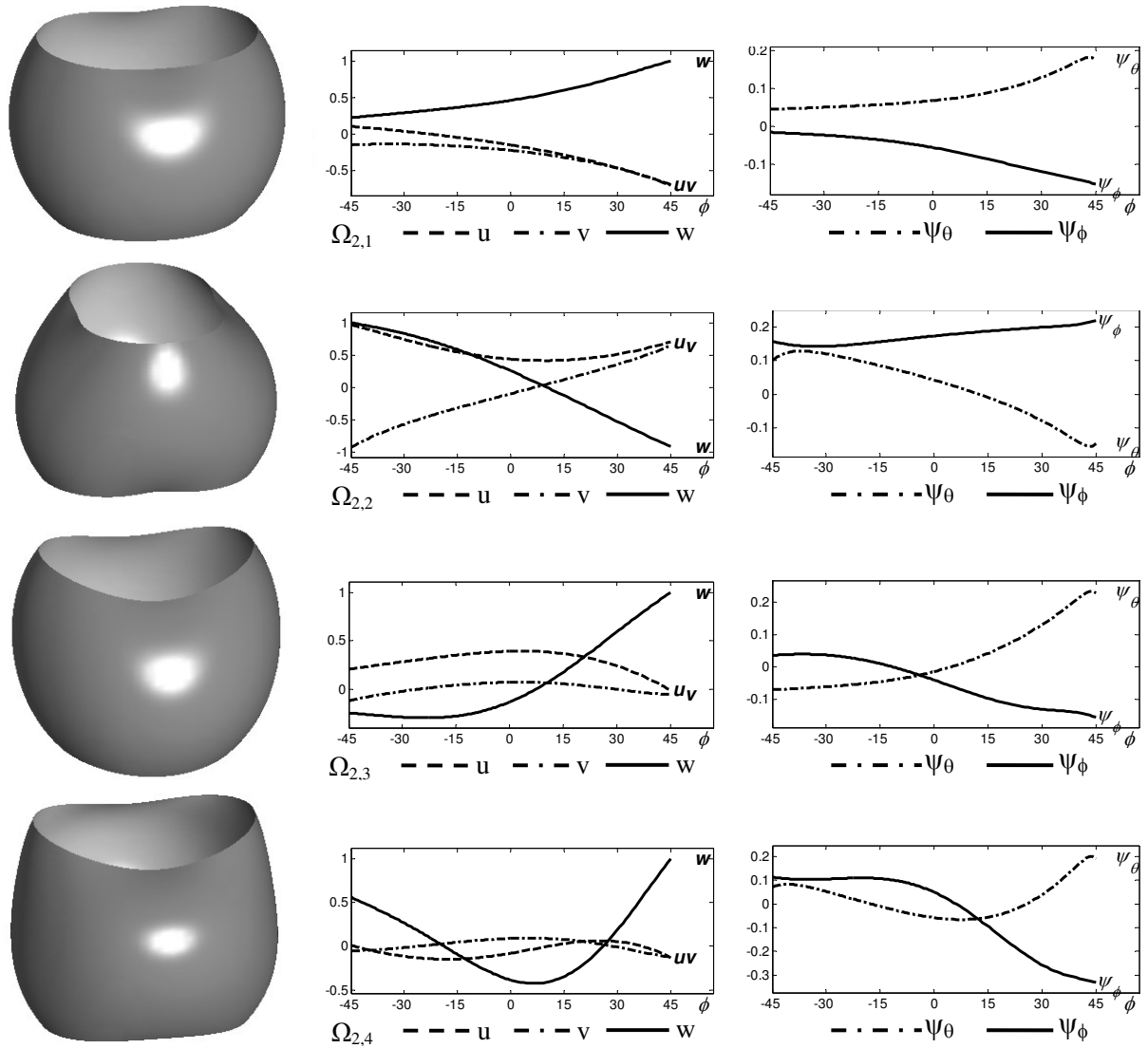
Figure 7. Mode shapes of vibrations with two circumferential waves ($n = 2$) of a completely free spherical barrel shell with variable thickness (Figure 3, right).

problem is a highly accurate solution (depending only on the accuracy of the numerical calculations).

(4) The order of the frequency determinants which are required for the solution by the present method are at least an order of magnitude smaller than those needed by a finite element analysis of comparable accuracy.

(5) The derived dynamic stiffness matrix allows combination of spherical shell segments into complex assemblies with different combinations of shell types, variable thickness, and analyzing them with small number of elements.

Appendix: Entries of the coefficient matrices $K^{(0)}$, $K^{(1)}$, and $K^{(2)}$ in Equation (14)

Only nonzero entries are listed. We set $\Phi = 1/\phi_0$.

$K_{11}^{(0)} = \omega^2(\rho/E)(1-\mu^2)R_p^2 R_0^3 h + R_p R_0(R_p' h' + R_p'' h)\Phi^2 \mu - \frac{1}{2}(1-\mu)(R_p^2 R_0 \kappa h + R_0^3 h n^2)$

$K_{12}^{(0)} = \frac{1}{2}R_0^2 n \Phi R_p' h(\mu-3) + R_0^2 n \Phi R_p h' \mu$

$K_{13}^{(0)} = R_p^2 R_0 h' \Phi(1+\mu)$ $K_{14}^{(0)} = \frac{1}{6}\omega^2(\rho/E)(1-\mu^2)R_p^2 R_0^2 h^3 + \frac{1}{2}(1-\mu)R_p^2 R_0^2 \kappa h$

$K_{21}^{(0)} = \frac{1}{2}R_0^2 n \Phi R_p' h(\mu-3) - \frac{1}{2}R_0^2 n \Phi(1-\mu)R_p h'$

$K_{22}^{(0)} = \omega^2(1-\mu^2)(\rho/E)R_p^2 R_0^3 h - \frac{1}{2}(1-\mu)R_p R_p'' R_0 h \Phi^2 \mu - \frac{1}{2}(1-\mu)R_p R_p' R_0 h' \Phi^2 - R_0^3 h n^2$
$$\qquad\qquad\qquad\qquad\qquad -\frac{1}{2}(1-\mu)R_p^2 R_0 \kappa h - \frac{1}{2}(1-\mu)R_p'^2 R_0 h \Phi^2$$

$K_{23}^{(0)} = -(1+\mu)R_p R_0^2 h n - \frac{1}{2}(1-\mu)R_p R_0^2 \kappa h n$ $K_{25}^{(0)} = \frac{1}{6}\omega^2(\rho/E)(1-\mu^2)R_p^2 R_0^2 h^3 + \frac{1}{2}(1-\mu)R_p^2 R_0^2 \kappa h$

$K_{31}^{(0)} = -(1+\mu)R_p R_p' R_0 \Phi h - \frac{1}{2}(1-\mu)R_p R_p' R_0 \kappa h \Phi - \frac{1}{2}(1-\mu)R_p^2 R_0 \kappa h' \Phi$

$K_{32}^{(0)} = K_{23}^{(0)}$ $K_{33}^{(0)} = \omega^2(\rho/E)(1-\mu^2)R_p^2 R_0^3 h - \frac{1}{2}(1-\mu)R_0^3 \kappa h n^2 - 2(1+\mu)R_p^2 R_0 h$

$K_{34}^{(0)} = \frac{1}{2}(1-\mu)\left(R_p^2 R_0^2 \kappa h' + R_p R_p' R_0^2 \Phi \kappa h\right)$ $K_{35}^{(0)} = \frac{1}{2}(1-\mu)R_p R_0^3 \kappa h n$

$K_{41}^{(0)} = K_{14}^{(0)}$

$K_{44}^{(0)} = \frac{1}{12}\omega^2(\rho/E)(1-\mu^2)R_p^2 R_0^3 h^3 - \frac{1}{24}(1-\mu)R_0^3 h^3 n^2 - \frac{1}{12}R_p'^2 R_0 h^3 \Phi^2(1+\mu)$
$$\qquad\qquad\qquad -\frac{1}{2}(1-\mu)R_p^2 R_0^3 \kappa h + \frac{1}{12}R_p R_p'' R_0 h^3 \Phi^2 \mu + \frac{1}{4}R_p R_p' R_0 h' h^2 \Phi^2 \mu$$

$K_{45}^{(0)} = \frac{1}{4}n\mu R_p R_0^2 h' h^2 \Phi - \frac{1}{24}R_p' R_0^2 n \Phi h^3(3-\mu)$

$K_{52}^{(0)} = K_{25}^{(0)}$ $K_{53}^{(0)} = K_{35}^{(0)}$ $K_{54}^{(0)} = -\frac{1}{8}(1-\mu)n R_p R_0^2 h' h^2 \Phi - \frac{1}{24}R_p' R_0^2 n \Phi h^3(3-\mu)$

$K_{55}^{(0)} = \frac{1}{12}\omega^2(\rho/E)(1-\mu^2)R_p^2 R_0^3 h^3 + \frac{1}{24}(1-\mu)R_p R_p'' R_0 h^3 \Phi^2 + \frac{1}{8}(1-\mu)R_p R_p' R_0 h' h^2 \Phi^2 \mu$
$$\qquad\qquad\qquad -\frac{1}{2}(1-\mu)R_p^2 R_0^3 \kappa h - \frac{1}{12}R_0^3 n^2 h^3 - \frac{1}{12}R_p'^2 R_0 h^3 \Phi^2(1-\mu)$$

$K_{11}^{(1)} = R_p R_p' R_0 h \Phi^2 + R_p^2 R_0 h' \Phi^2$

$K_{12}^{(1)} = \frac{1}{2}(1+\mu)R_p R_0^2 h n \Phi$ $K_{13}^{(1)} = (1+\mu)R_p^2 R_0 \Phi h + \frac{1}{2}(1-\mu)R_p^2 R_0 K \Phi h$

$K_{21}^{(1)} = -K_{12}^{(1)}$ $K_{22}^{(1)} = \frac{1}{2}(1-\mu)R_p R_p' R_0 h \Phi^2 + \frac{1}{2}(1-\mu)R_p^2 R_0 h' \Phi^2$

$K_{31}^{(1)} = -K_{13}^{(1)}$

$K_{33}^{(1)} = \frac{1}{2}(1-\mu)(R_p^2 R_0 \kappa h' \Phi^2 + R_p R_p' R_0^2 \Phi^2 \kappa h)$ $K_{34}^{(1)} = \frac{1}{2}(1-\mu)R_p^2 R_0^2 \kappa h \Phi$

$K_{43}^{(1)} = K_{34}^{(1)}$

$K_{44}^{(1)} = \Phi^2 R_0\left(\frac{1}{12}R_p R_p' h^3 + \frac{1}{4}R_p^2 h' h^2\right)$ $K_{45}^{(1)} = \frac{1}{24}(1+\mu)R_p R_0^2 \Phi h^3 n$

$K_{54}^{(1)} = -K_{45}^{(1)}$ $K_{55}^{(1)} = \frac{1}{8}(1-\mu)2\Phi^2 R_p^2 R_0 h' h^2 + \frac{1}{24}(1-\mu)R_p R_p' R_0 h^3 \Phi^2$

$$K_{11}^{(2)} = R_p^2 R_0 h \Phi^2$$
$$K_{22}^{(2)} = \tfrac{1}{2}(1-\mu) R_p^2 R_0 h \Phi^2$$
$$K_{33}^{(2)} = \tfrac{1}{2}(1-\mu) R_p^2 R_0 \kappa h \Phi^2$$
$$K_{44}^{(2)} = \tfrac{1}{12} R_p^2 R_0 \Phi^2 h^3$$
$$K_{55}^{(2)} = \tfrac{1}{24}(1-\mu) R_p^2 R_0 \Phi^2 h^3$$

References

[Eisenberger 1990] M. Eisenberger, "An exact element method", *Int. J. Numer. Methods Eng.* **30** (1990), 363–370.

[Gautham and Ganesan 1992] B. P. Gautham and N. Ganesan, "Free vibration analysis of thick spherical shells", *Comput. Struct.* **2**:45 (1992), 307–313.

[Hutchinson 1984] J. R. Hutchinson, "Vibrations of thick free circular plates, exact versus approximate solutions", *J. Appl. Mech. (ASME)* **51** (1984), 581–585.

[Kang and Leissa 2000] J. H. Kang and A. W. Leissa, "Three-dimensional vibrations of thick spherical shell segments with variable thickness", *Int. J. Solids Struct.* **37** (2000), 4811–4823.

[Kang and Leissa 2006] J. H. Kang and A. W. Leissa, "Corrigendum to Three-dimensional vibrations of thick spherical shell segments with variable thickness", *Int. J. Solids Struct.* **43** (2006), 2848–2851.

[Leissa 1973] A. W. Leissa, *Vibrations of shells*, US Government Printing Office, 1973. Reprinted Acoustical Soc. Amer., New York, 1993.

[Leissa and Chang 1996] A. W. Leissa and J. D. Chang, "Elastic deformation of thick, laminated composite shells", *Compos. Struct.* **35** (1996), 153–170.

[Lim et al. 1996] C. W. Lim, S. Kitipornchai, and K. M. Liew, "Modeling the vibration of a variable thickness ellipsoidal dish with central point clamp or concentric surface clamp", *J. Acoust. Soc. Am.* **I**:99 (1996), 362–372.

[Mindlin 1951] R. D. Mindlin, "Influence of rotatory inertia and shear on flexural motions of isotropic, elastic plates", *J. Appl. Mech. (ASME)* **18** (1951), 31–38.

[Qatu 2002] M. S. Qatu, "Recent research advances in the dynamic behavior of shells: 1989–2000, Part 2: Homogeneous shells", *Appl. Mech. Rev.* **5**:55 (2002), 415–434.

[Stephen 1997] N. G. Stephen, "Mindlin plate theory: best shear coefficient and higher spectra validity", *J. Sound Vib.* **202**:4 (1997), 539–553.

ELIA EFRAIM: efraime@ariel.ac.il
Department of Civil Engineering, Ariel University Center of Samaria, 40700 Ariel, Israel

MOSHE EISENBERGER: cvrmosh@technion.ac.il
Faculty of Civil and Environmental Engineering, Technion – Israel Institute of Technology, Technion City, 32000 Haifa, Israel

JOURNAL OF MECHANICS OF MATERIALS AND STRUCTURES

http://www.jomms.org

Founded by Charles R. Steele and Marie-Louise Steele

Cover design: Alex Scorpan   Cover photo: Wikimedia Commons

See inside back cover or http://www.jomms.org for submission guidelines.

PUBLISHED BY
■ mathematical sciences publishers
http://www.mathscipub.org
A NON-PROFIT CORPORATION
Typeset in LaTeX

Journal of Mechanics of Materials and Structures

Volume 5, No. 5   May 2010